

Nonisothermal Cure Kinetics of DGEBA with Novel Aromatic Diamine

M. Ghaemy, M. Barghamadi, H. Behmadi

Department of Chemistry, Mazandaran University, Babolsar, Iran

Received 15 July 2006; accepted 31 August 2006

DOI 10.1002/app.25473

Published online in Wiley InterScience (www.interscience.wiley.com).

ABSTRACT: The effect of the molar ratio of diglycidyl ether of a bisphenol-A based epoxy (DGEBA) and synthesized 4-phenyl-2,6-bis(4-aminophenyl)pyridine (PAP) as curing agent during nonisothermal cure reaction by the Kissinger, Ozawa, and isoconversional equations was studied. The cure mechanism was studied by FTIR analysis. Kinetic analysis of the curing reaction of DGEBA at two different concentrations (42 and 32 phr) of the curing agent was studied by using DSC analysis. With an increasing PAP content, the pre-exponential factor increased by

increasing collision probability between epoxide and primary or secondary amine groups in noncatalytic or catalytic modes. The activation energy also increased because of the increasing content of crosslink density. The activation energies obtained from three equations were in good agreement. © 2006 Wiley Periodicals, Inc. *J Appl Polym Sci* 103: 3076–3083, 2007

Key words: curing of polymers; kinetics; DSC; resins; FTIR

INTRODUCTION

Epoxy thermosets have been widely used as high-performance adhesives, barrier films in food packing, matrix resins in fiber-reinforced compositions, and matrix resins for composites due to their outstanding mechanical and thermal properties. These properties include high modulus and tensile strength, high glass transition temperature, high thermal stability, and moisture resistance. When cured, epoxy resins form a highly crosslinked three-dimensional infinite network whose microstructure leads to desirable engineering properties. The properties of a thermosetting polymer depend on the extent of chemical reactions that take place during cure and the resin morphology. To predict the morphology developed by the phase separation of rubber-rich phase during polymerization of epoxy resin with amines, it is necessary to know the reaction kinetics of the crosslinked polymer system. Although the chemistry involved in the epoxy curing process is rather complex, understanding the mechanisms and kinetics of the cure reactions is essential for a better knowledge of structure–property relationships. Curing kinetics models are generally developed by analyzing experimental results obtained by differential thermal analysis techniques. DSC in both isothermal and dynamic modes has been used extensively

in studying kinetics of cure reaction of epoxy with different curing agent systems.^{1–12} Many equations were developed to investigate the cure kinetics of the epoxy system, including the *n*th-order reaction model, the autocatalytic reaction model, and the diffusion control model.^{13–16} All kinetic models start with the following basic equation:

$$\frac{d\alpha}{dt} = kf(\alpha) \quad (1)$$

or in the integrated form,

$$g(\alpha) = \int \frac{d\alpha}{f(\alpha)} = \int k dt \quad (2)$$

where $d\alpha/dt$ is the instant cure rate, α is the fractional conversion at a time t , k is the Arrhenius rate constant, and $f(\alpha)$ is a functional form of α that depends on the reaction mechanism.

Kissinger derived the following equation^{13,17} for when the temperature varies with time at a constant heating rate, $q = dT/dt$:

$$-\ln(q/T_p^2) = E/RT_p - \ln(AR/E) \quad (3)$$

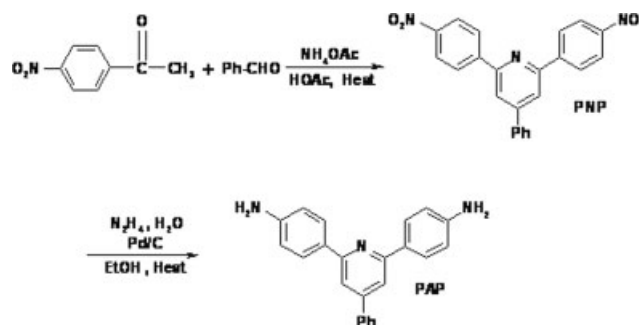
where q is the heating rate, T_p is the temperature at which $d\alpha/dt$ is maximum, E is the activation energy, R is the gas constant, and A is the pre-exponential factor. This method gives a relatively accurate activation energy and pre-exponential factor by calculating the relationship between $-\ln(q/T_p^2)$ and $1/T_p$.

Correspondence to: M. Ghaemy (ghaemy@umz.ac.ir).

TABLE I
Yield, Melting Point, and Spectroscopic Data of Curing Agent

Compounds	Yield (g)	M.p. (°C)	FTIR (cm ⁻¹)	¹ H-NMR (ppm)	Elemental analysis			
					%C	%H	%N	%O
PNP	14.75 (61.53%)	316–318	3035, 1600, 1447, 1510, 1355, 1105, 1005, 850, 825, 750, 685, 630	6.8–8.2(C–H aromatic, 15H)	69.10 (69.52) ^a	3.50 (3.78)	10.80 (10.58)	16.60 (16.12)
PAP	10.62 (91.00%)	205–207	3410, 3336, 3216, 1620, 1600, 1537, 1509, 1445, 1396, 1283, 1248, 1170, 824, 754, 690	7.0–8.2 (C–H aromatic, 15H); 3.99 (NH ₂ , 4H)	81.85 (81.90)	5.57 (5.64)	12.58 (12.46)	–

^a Requested values are shown in parentheses.



Scheme 1 Chemical structures of materials.

The Kissinger equation gives only one activation energy from the data of T_p . A more complete determination of the activation energy at any selected conversion can be calculated using the isoconversional equation¹⁶:

$$E = -R \frac{d(\ln q)}{d(T^{-1})} \quad (4)$$

Where E , q , and R are the same terms as in the Kissinger equation and T is the temperature for a selected conversion at each heating rate. Activation energies can be obtained from the slope.

Ozawa-Flynn-Wall method based on Doyle's approximation^{18,19} is an alternative method for the calculation of activation energy and is expressed as follows:

$$\ln q = 1/2.303 \ln q = -0.4567E_a/RT_p + (\log AE_a/R - \log f(\alpha) - 2.315) \quad (5)$$

A plot of $\ln(q)$ versus $(1/T_p)$ should give a straight line with a slope of $-1.052E_a/R$. This can provide activation energy for different levels of conversion.

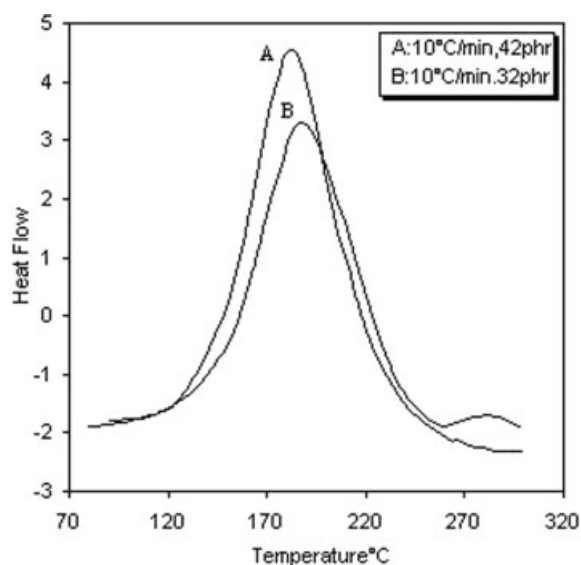
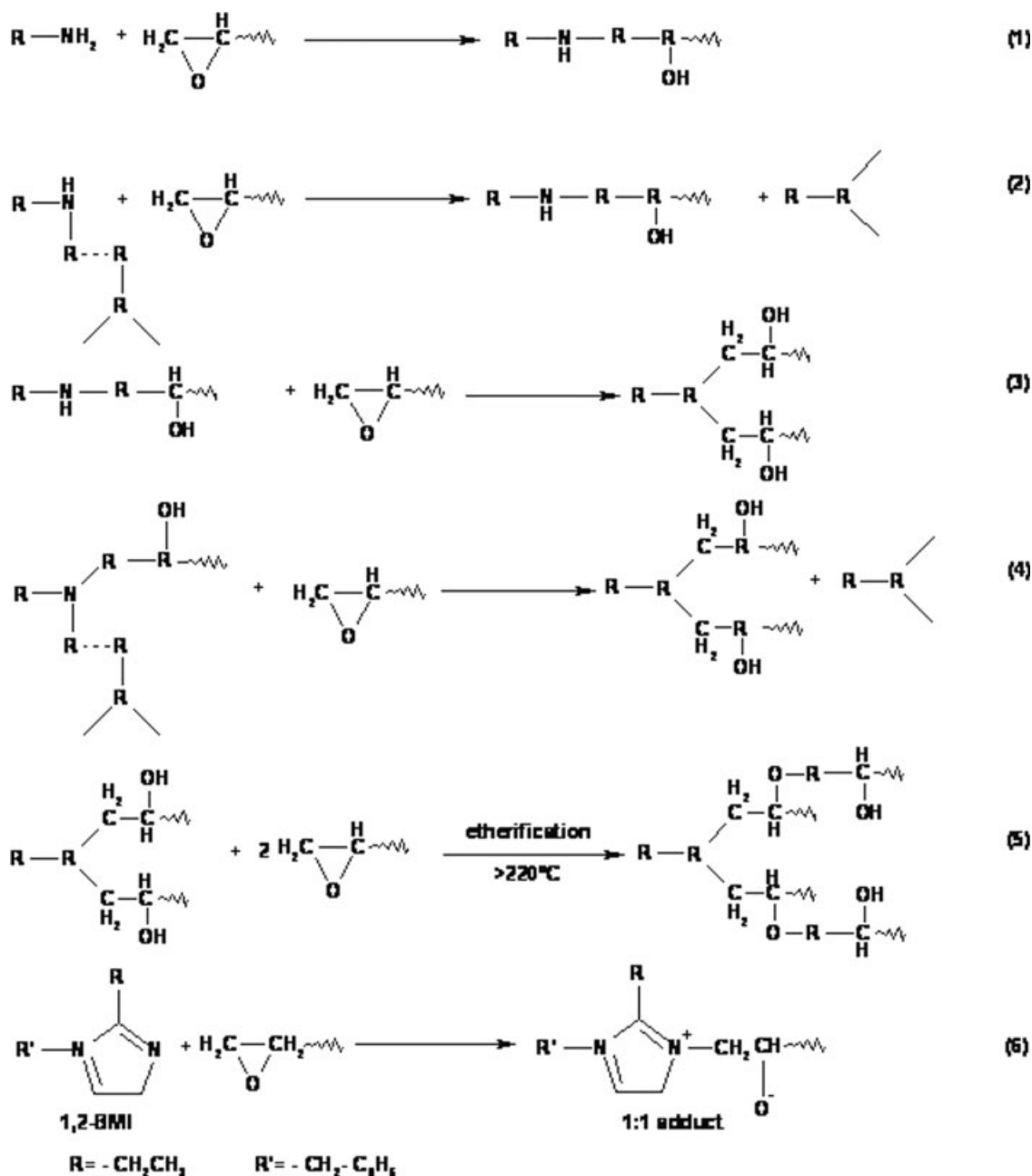


Figure 1 Typical dynamic DSC thermograms of DGEBA/PAP system.



Scheme 2 Proposed mechanism of cure reaction of DGEBA.

In this work, first the aromatic diamine (PAP) was synthesized and characterized according to the procedure given in the literature. The cure reaction of PAP, which has not been used as a curing agent before, and epoxy monomer (DGEBA) at various molar ratios was investigated by using nonisothermal DSC techniques. To calculate the kinetic parameters, DSC data under dynamic conditions were introduced to the Kissinger, Ozawa, and isoconversional equations. The cure reaction mechanism was also confirmed by FTIR analysis.

EXPERIMENTAL

Apparatus

A Mettler Toledo differential scanning calorimeter (DSC822^e) was used to monitor the exothermic thermograms of crosslinking reaction. The FTIR used was Bruker, Vector 22. The FTIR spectra of the synthesized curing agent and curing reaction were obtained using KBr pellets. The ¹H-NMR spectra were recorded on a Bruker Avance DPX 250 MHz instrument, using DMSO-*d*₆ as solvent. Elemental analysis

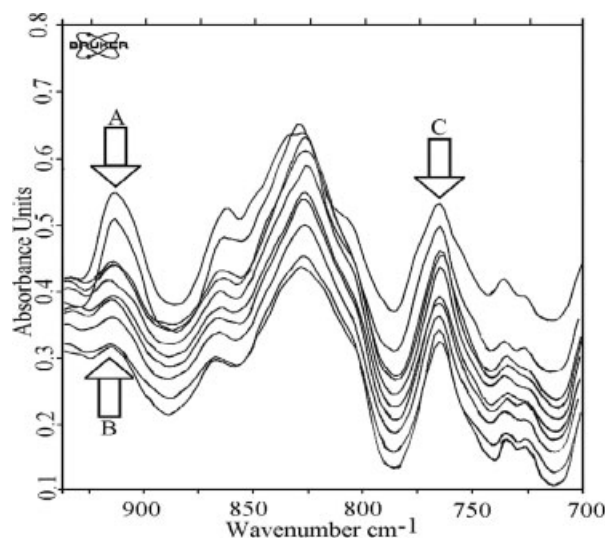


Figure 2 FTIR spectra of mixture of DGEBA and 42 phr PAP during cure for 30 min at 180°C.

(carbon and nitrogen) was performed with CHN-600 Leco.

Materials

The epoxy compound used in the study was a diglycidyl ether of a bisphenol A (DGEBA)-based epoxy, Epidian5: Epoxide equivalent 196–208, clear yellow liquid, viscosity (at 25°C) 25,000 mpas, provided from Iran Petrochemical Industry. Other compounds such as *p*-nitroacetophenone, ammonium acetate, glacial acetic acid, Pd/C 5%, hydrazinehydrate 85%, and ethanol were obtained from Fluka and used without further purification. Benzaldehyde was also received from Fluka and purified with vacuum distillation.

Synthesis

4-Phenyl-2,6-bis(4-nitrophenyl) pyridine

This compound was synthesized according to the following procedure.²⁰ In a round-bottomed flask (250 mL) equipped with a reflux condenser, a mixture of benzaldehyde (6.4 g, 0.06 mol), *p*-nitroacetophenone (20 g, 0.12 mol), ammonium acetate (60 g), and glacial acetic acid (150 mL) was refluxed for 2 h. Upon cooling, crystals separated, which were filtered and washed first with acetic acid (50%) and then with cold ethanol. These dark yellow crystals were recrystallized from absolute ethanol, and then dried at 60°C under vacuum. The product was 4-phenyl-2,6-bis(4-nitrophenyl) pyridine (PNP). The yield and other characteristics are shown in Table I.

4-Phenyl-2,6-bis(4-aminophenyl) pyridine

In a two-necked round-bottomed flask (1000 mL) equipped with a reflux condenser and a dropping

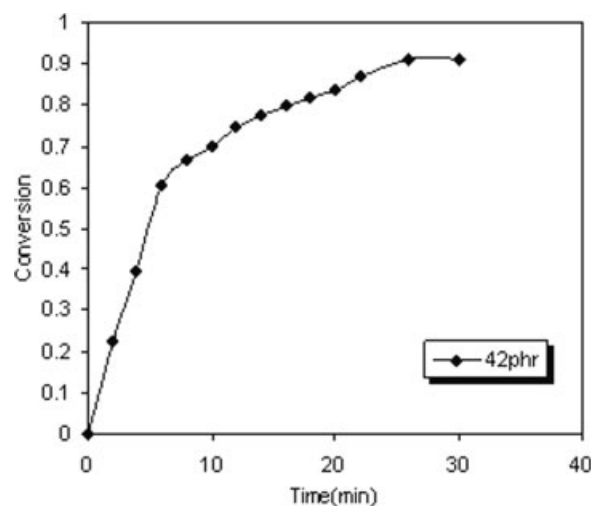


Figure 3 Conversion against time for DGEBA cured with 42 phr PAP at 180°C.

funnel, a suspension of 4-phenyl-2,6-bis(4-nitrophenyl) pyridine (PNP) (13.75 g, 0.033 mol), palladium on carbon 5% (1.4 g), and ethanol (500 mL) was prepared. The mixture was warmed, and while being stirred magnetically, hydrazine hydrate 85% (35 mL) in ethanol (50 mL) was added dropwise over a 1.5 h period through the dropping funnel while maintaining the temperature at about 50°C. The reaction mixture was then refluxed for 2 h and filtered while hot. On cooling, the filtrate gave white-cream colored crystals of the title diamine compound, which were recrystallized from ethanol and vacuum dried (Scheme 1). Yield and other data are shown in Table I.

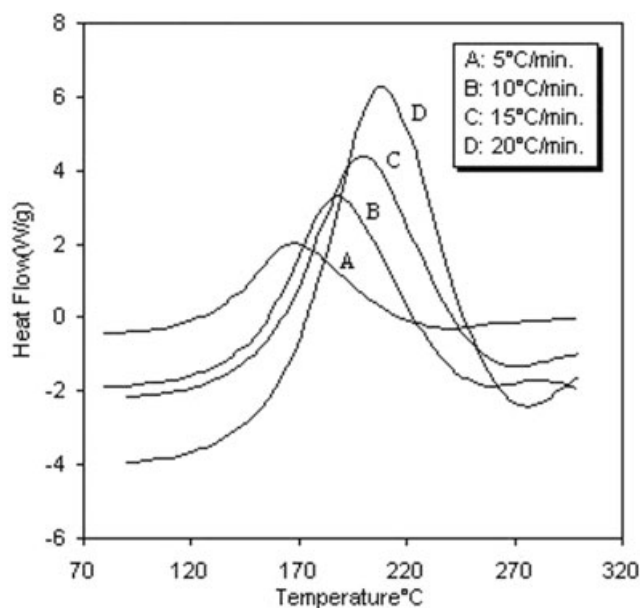


Figure 4 Dynamic DSC thermograms for DGEBA cured with 32 phr PAP at different heating rates.

TABLE II
DSC Data for DGEBA Cured at Different Concentrations and Heating Rates

Concentration (phr)	q ($^{\circ}\text{C}/\text{min}$)	T_p (K)	$1/T_p \times 10^3$ (K^{-1})	$\ln q$	$-\ln(q/T_p^2)$	Exothermic heat (J/g)
32	5	441.41	2.265	1.61	10.57	46.10
	10	460.98	2.169	2.30	9.96	96.35
	15	472.62	2.116	2.71	9.61	167.24
	20	481.14	2.078	3.00	9.36	190.66
42	5	438.33	2.281	1.61	10.56	56.21
	10	455.37	2.196	2.30	9.94	138.37
	15	468.93	2.132	2.71	9.59	199.07
	20	475.81	2.102	3.00	9.33	211.93

Sample mixing

The stoichiometric amounts of the curing agent were calculated through the number of active amino hydrogens in PAP. For instance, PAP has a molar mass of 337 g/mol and contains four active hydrogen atoms. Therefore, 1 mol of active hydrogen atoms represents 84.25 g of PAP. This figure is in the stoichiometric equivalent of the eew, and hence, for every 200 g of DGEBA, 84.25 g PAP (~ 42 wt %) as curing agent was required. Samples of DGEBA containing the required amounts of curing agents were completely mixed by stirring at room temperature. The mixtures were stored in a refrigerator until used for further investigation.

DSC analysis

A 5–6 mg of the uniform viscous liquid was put into a DSC sample pan and covered with an aluminum lid and closed tightly under pressure. The sample pan was placed in the DSC sample cell at ambient temperature, and an empty pan was also placed in the DSC reference cell, and it was heated according to the program of a constant heating rate from room temperature to 300 $^{\circ}\text{C}$. The heating rates were 5, 10, 15, and 20 $^{\circ}\text{C}/\text{min}$ under nitrogen purge.

FTIR analysis

FTIR analysis was carried out to study the mechanism of cure reaction between DGEBA and PAP. The mixed sample was cured at a constant temperature (180 $^{\circ}\text{C}$) for various times, and the partially cured sample was analyzed by using FTIR spectroscopy from 4000 to 700 cm^{-1} . The characteristic band for epoxide group at 916 cm^{-1} (spectrum A in Fig. 2) was recorded and compared with mono-substituted benzene absorption peak at 765 cm^{-1} (spectrum C).

RESULTS AND DISCUSSION

Figure 1 shows dynamic DSC curves for DGEBA cured with synthesized PAP at two different molar ratios and at the same heating rate. The exothermic

peaks with an almost 5 $^{\circ}\text{C}$ difference in the maximum were attributed to the generation of heat during the cure reaction. The functional groups are almost freely movable, as PAP is completely soluble in the resin at temperatures above 50 $^{\circ}\text{C}$ and it results in a rapid reaction. The exothermic peak showed a very steep slope, meaning that the cure reaction took place rapidly in a short temperature range. The exotherm is mainly caused by the sum of the reactions shown in Scheme 2: (a) Noncatalytic or catalytic reactions between primary amines of PAP [Reactions (1) and (2)] and produced secondary amines [Reactions (3) and (4)] with epoxide groups yield secondary and tertiary amines and hydroxyl groups. The hydroxyl groups which act as catalyst are present in the initial epoxy molecules or produced during epoxide ring opening reaction. (b) The etherification reactions [Reaction (5)], which may be neglected for stoichiometric mixtures of epoxy with diamines because the reactivity of the diamines to the epoxide rings is much higher than the hydroxyl groups, can be significant when diamine is lower than the stoichiometric value especially at temperatures > 220 $^{\circ}\text{C}$. (c) PAP can initiate formation of adduct according to the mechanism suggested in the literature,¹² for the reaction between epoxide group and the more basic pyridine-type nitrogen in 1-substituted imidazole [Reaction (6)]. However, there is no indication of occurrence of such reaction in this case because of the absence of low temperature shoulder in DSC thermogram, which was seen for 1-substituted imidazole, and also because of the high reactivity of the diamines to the epoxide groups in comparison with the reactivity of pyridine-type nitrogen, which can be also neglected when diamine is used in stoichiometric amount.

The mechanism of cure reaction was confirmed by FTIR analysis. Figure 2 shows the FTIR spectra of DGEBA cured with 42 phr PAP in the oven at 185 $^{\circ}\text{C}$ from 0 (spectrum A) to 30 min (spectrum B). It is well known that the phenylene group does not take part in the chemical reaction during the cure of the system; so the absorption peak at 765 cm^{-1} of mono-substituted benzene ring was taken as a reference peak for the normalization of the epoxy absorption peak. In spectrum A, the characteristic band of the

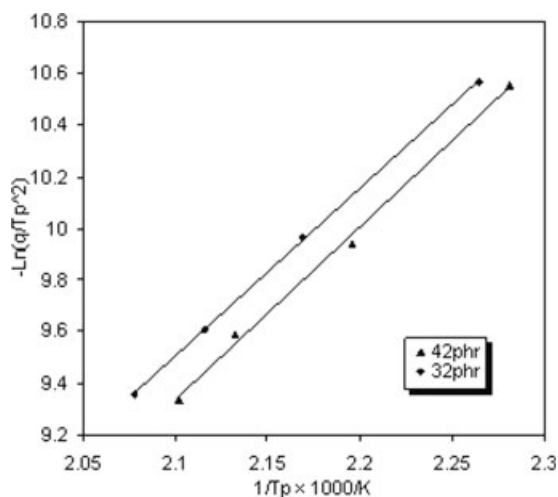


Figure 5 Kissinger plots for DGEBA/PAP system.

epoxy ring vibration of DGEBA appeared at 916 cm^{-1} , and as the cure reaction proceeded, this characteristic band of the epoxy ring decreased and disappeared completely at the end of the cure reaction. The epoxide group conversion against cure time, which has been calculated according to the eq. (6) from FTIR spectra, is shown in Figure 3.

$$[E]_t = \frac{[A]_t}{[B]_t} \quad \text{and} \quad \alpha = \frac{[E]_0 - [E]_t}{[E]_0} \quad (6)$$

where $[A]_t$ and $[B]_t$ are the area under the peaks of 916 and 765 cm^{-1} , respectively, and $[E]$ denotes the concentration of epoxide group at time t and the subscript 0 denotes time $t = 0$.

The initial slope of the curve in Figure 3 was steeper, but next to that, the slope get smaller after a certain amount of time, which could have been due to a diffusion-controlled reaction.²¹ The degree of conversion (α), Figure 3, showed autoacceleration in the initial stages, as indicated by the slight positive curvature. Curing thermosetting materials that generally involves transition of low molecular weight in liquid or rubbery state to an amorphous glassy state with infinite molecular weight is called vitrification. The chemical kinetics in the region near vitrification is often complicated by diffusion and/or mobility control. In principal, the reaction can proceed to a point ($T_g > T_{\text{cure}}$) where all chain movement ceases

and the reaction arrests because of the complete absence of mobility. This leads to a final conversion lower than unity in diffusion controlled conditions. The ultimate conversion can also be lower because the remaining reactive groups can not meet and react even in the absence of any diffusion hindrance.

Figure 4 shows dynamic DSC curves for DGEBA cured with 32 phr PAP at four different heating rates. All curves showed only one sharp exothermic peak, regardless of the heating rate. The exothermic peaks became larger and sharper and also shifted toward higher temperatures as heating rate was increased. Table II shows that the maximum temperature of the exothermic peaks shifted to the lower temperatures with the increasing concentration of PAP and shifted to the higher temperatures with the increasing heating rate. Table II also shows the increasing heat generation with the increasing heating rate and also with the increasing concentration of PAP. At a higher percentage of PAP, the probability of the exothermic reaction between the epoxide and amine groups at a lower temperature increased; at a higher heating rate, the exothermic reaction occurred at the higher temperatures with the less-arranged molecules, and the lower crosslink network made the mobility of the functional groups easy, and as a natural consequence, the exothermic heat increased. The temperature at which the instant conversion rate was maximum (T_p) and the heating rate (q) (Table II) were used for calculation of kinetic parameters by using Kissinger, Ozawa, and isoconversional methods.

The data in the fourth and sixth columns of Table II were introduced to the Kissinger equation, and $-\ln(q/T_p^2)$ versus $1/T_p$ is plotted in Figure 5. The linear plots are expressed by the following equations for 32 and 42 phr of PAP, respectively:

$$-\ln(q/T_p^2) = 6.48 \times 10^3(1/T_p) - 4.11 \quad (32 \text{ phr})$$

and

$$-\ln(q/T_p^2) = 6.64 \times 10^3(1/T_p) - 4.62 \quad (42 \text{ phr})$$

The activation energies were calculated from the slope and the pre-exponential factors from the y intersect, and these values were listed in Table III. As the weight percent of PAP as the curing agent was increased (from 32 to 42 phr), the activation

TABLE III
Values of Kinetic Parameters of DGEBA Cured with Different Heating Rates

Concentration (phr)	E_a (kJ/mol)		A (min^{-1})	K (min^{-1}) ^a
	Kissinger's method	Ozawa's method		
32	53.89	58.49	3.94×10^5	0.24
42	55.22	59.76	6.78×10^5	0.29

^a Arrhenius rate constant at 453 K.

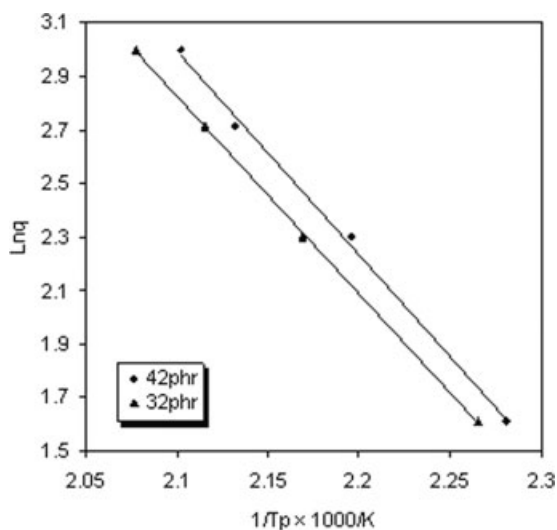


Figure 6 Ozawa plots for DGEBA/PAP system.

energy and the pre-exponential factor increased slightly. The increase in the pre-exponential factor is due to the increasing probability of collision between reactant groups. The slight increase in the activation energy can be attributed to the increasing content of high crosslink density which ceased the diffusion of functional groups. To compare the cure rate of the two systems, pre-exponential factor and activation energy values are introduced to the following Arrhenius equation to get rate constants at a selected temperature, and the data are shown in Table III.

$$k = A \exp(-E_a/RT)$$

where k is the rate constant and T is a selected temperature (453 K). The rate constant for DGEBA/PAP system also increased as the weight percent of PAP increased.

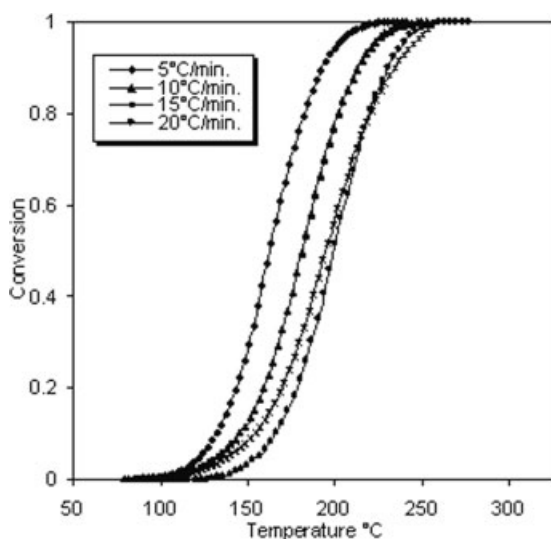


Figure 7 Conversion curves at different heating rates for DGEBA cured with 32 phr PAP.

TABLE IV
Data of $\ln(q)$ and T^{-1} for 32 phr DGEBA/PAP System

$\ln q$	$1/T_p \times 10^3 \text{ (K}^{-1}\text{)}$				
	0.1	0.2	0.3	0.4	0.5
1.61	2.46	2.40	2.36	2.32	2.29
2.30	2.39	2.31	2.26	2.23	2.20
2.71	2.34	2.26	2.21	2.17	2.14
3.00	2.28	2.21	2.17	2.14	2.12

The data in fourth and fifth columns of Table II were also introduced into the Ozawa equation, and plot of $\ln(q)$ versus $(1/T_p)$ gave a straight line with a slope of $-1.052E_a/R$, as shown in Figure 6, and the activation energies calculated from the slope were listed in Table III.

Figure 7 shows the conversion curves at four different heating rates for DGEBA cured with 32 phr of PAP. These curves were obtained by integrating the DSC curves in Figure 4. The isoconversional temperatures were obtained from the conversion curves at any selected conversion, and $1/T \times 10^3$ according to $\ln(q)$ are listed in Table IV. To get the activation energy at each conversion, the relationships of the variables at the conversion of 0.1–0.5 were discerned (Fig. 8), and the linear expression for each straight line was obtained. All slopes corresponded to $-E/R$ at these particular conversions, and the activation energies are listed in Table V. This table also contains the activation energies at these particular conversions for DGEBA cured with 42 phr of PAP. The values increased slightly with increasing conversion, which can be due to restriction in the diffusion of functional groups. The average reaction values of the activation energies for the curing reaction of DGEBA with

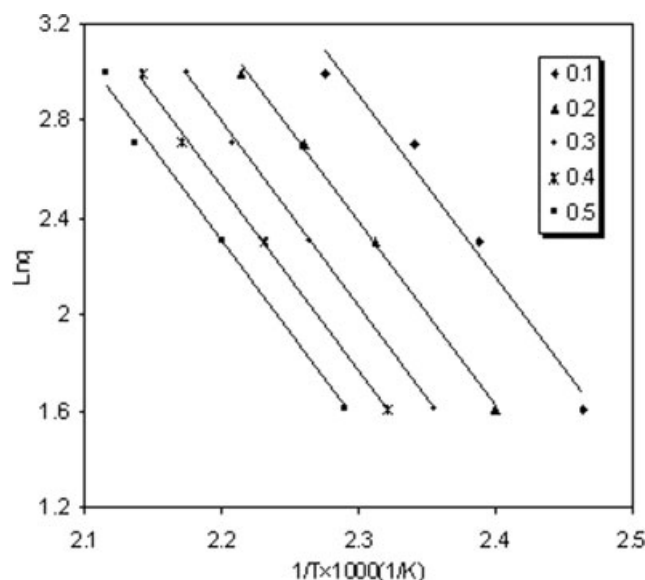


Figure 8 Isoconversional plots at various conversions for the 32 phr DGEBA/PAP system.

42 and 32 phr of PAP as curing agent were 64.49 and 62.86 kJ/mol, respectively.

The activation energies for the cure reaction of DGEBA/PAP system using data from DSC scans and three kinetic models (Kissinger, Ozawa, and isoconversional equations) are given in Table VI for comparison. Although the activation energies obtained by using these three methods increased from 55.2 to 59.7 and to 64.5 kJ/mol for DGEBA/PAP system, respectively, but the agreement between these values are reasonably good. The increase in activation energy with increasing the amount of PAP can be due to increasing content of high crosslink density, which hindered the diffusion of the reactant functional groups.

CONCLUSIONS

Mechanism and kinetics of the cure reaction of DGEBA with a new aromatic diamine PAP was studied by using DSC scanning technique with three kinetic models: Kissinger, Ozawa, and isoconversional equations and by FTIR analysis. All dynamic DSC curves showed only one sharp exothermic peak, regardless of the heating rate; this meant that the cure reactions between the epoxide groups and primary or secondary amine groups took place in the same stage. DSC thermogram shifted to lower temperature with increasing the amount of PAP and shifted to higher temperatures with increasing heating rate. As PAP content increased, the pre-exponen-

TABLE V
Activation Energy for DGEBA/PAP Systems with Different Molar Ratios by Isoconversional Equation

Concentration	Conversion	E_a (kJ/mol)	Average E_a (kJ/mol)
32	0.1	62.30	62.86
	0.2	62.52	
	0.3	62.97	
	0.4	63.13	
	0.5	63.31	
42	0.1	62.95	64.49
	0.2	63.75	
	0.3	64.48	
	0.4	65.59	
	0.5	65.72	

TABLE VI
Activation Energy for DGEBA/PAP Systems with Different Kinetics Model

Concentration	E_a (kJ/mol)		
	Kissinger's method	Ozawa's method	Isoconversional equation
32	53.89	58.49	62.86
42	55.22	59.76	64.49

tial factor was increased because of increasing probability of collision between the epoxide and amine groups. The activation energy also increased because of the increase in the content of crosslink density. The activation energies obtained from three kinetic methods were approximately in good agreement. The rate constant also increased with increasing the amount of curing agent PAP.

References

- Sourour, S.; Kamal, M. R. *Thermochem Acta* 1976, 14, 41.
- Mijovic, J.; Kim, J.; Slaby, J. *J Appl Polym Sci* 1984, 29, 1449.
- Enns, J. B.; Gillham, J. K. *J Appl Polym Sci* 1983, 28, 2567.
- Wisnarakit, G.; Gillham, J. K.; Enns, J. B. *J Appl Polym Sci* 1990, 41, 1895.
- Khanna, U.; Chanda, M. *J Appl Polym Sci* 1993, 49, 319.
- Deng, Y.; Martin G. C. *Macromolecules* 1994, 27, 5147.
- Girard-Rejdet, E.; Riccardi, C. C.; Sautereau, H.; Pasault, J. P. *Macromolecules* 1995, 28, 7599.
- Ghaemy, M.; Khandani, M. H. *Eur Polym J* 1998, 34(3/4), 477.
- Ghaemy, M.; Riahy, M. H. *Eur Polym J* 1996, 32, 1207.
- Ghaemy, M. *J Therm Anal Calorim* 2003, 72, 743.
- Ghaemy, M.; Barghamadi, M.; Behmadi, H. *J Appl Polym Sci* 2004, 94, 1049.
- Ghaemy, M.; Sadjady, S. *J Appl Polym Sci* 2006, 100, 2634.
- Gu, J.; Narang, S. C.; Pearce, E. M. *J Appl Polym Sci* 1985, 30, 2997.
- Keenan, M. R. *J Appl Polym Sci* 1987, 33, 1725.
- Lu, M. G.; Shim, M. J.; Kim, S. W. *Polym Eng Sci* 1999, 39, 274.
- Montserrat, S.; Flaque, C.; Pages, P.; Maek, J. *J Appl Polym Sci* 1995, 56, 1413.
- Kissinger, H. E. *Anal Chem* 1957, 29, 1702.
- Ozawa, T. *J Therm Anal Calorim* 1970, 2, 301.
- Moroni, A.; Mijovic, J.; Pearce, E.; Foun, C. C. *J Appl Polym Sci* 1986, 32, 3761.
- Tamami, B.; Yeganeh, H. *Polymer* 2001, 42, 415.
- Sewell, G. J.; Billingham, N. C.; Kozielski, K. A.; George G. A. *Polymer* 2000, 41, 2113.